



UNIVERSITÀ POLITECNICA DELLE MARCHE
Repository ISTITUZIONALE

Influence of EMG-signal processing and experimental set-up on prediction of gait events by neural network

This is the peer reviewed version of the following article:

Original

Influence of EMG-signal processing and experimental set-up on prediction of gait events by neural network / Di Nardo, F.; Morbidoni, C.; Cucchiarelli, A.; Fioretti, S.. - In: BIOMEDICAL SIGNAL PROCESSING AND CONTROL. - ISSN 1746-8094. - ELETTRONICO. - 63:(2021). [10.1016/j.bspc.2020.102232]

Availability:

This version is available at: 11566/291070 since: 2024-07-02T08:16:36Z

Publisher:

Published

DOI:10.1016/j.bspc.2020.102232

Terms of use:

The terms and conditions for the reuse of this version of the manuscript are specified in the publishing policy. The use of copyrighted works requires the consent of the rights' holder (author or publisher). Works made available under a Creative Commons license or a Publisher's custom-made license can be used according to the terms and conditions contained therein. See editor's website for further information and terms and conditions.

This item was downloaded from IRIS Università Politecnica delle Marche (<https://iris.univpm.it>). When citing, please refer to the published version.

note finali coverpage

(Article begins on next page)

1 **Influence of EMG-signal processing and experimental set-up on**
2 **prediction of gait events by neural network**

3
4 Francesco DI NARDO¹, Christian MORBIDONI¹,
5 Alessandro CUCCHIARELLI¹, Sandro FIORETTI¹

6
7
8
9 ¹ Department of Information Engineering, Università Politecnica delle Marche,
10 via Brece Bianche, 60131 Ancona, Italy.

11
12
13
14 **Corresponding author:**

15 Francesco Di Nardo, Ph.D.

16 Department of Information Engineering

17 Università Politecnica delle Marche

18 Via Brece Bianche, 60131 Ancona, Italy

19 Fax: (39)0712204224; e-mail: f.dinardo@staff.univpm.it

26 **Abstract**

27 Machine-learning approaches are satisfactorily implemented for classifying and assessing
28 gait events from only surface electromyographic (sEMG) signals during walking.
29 However, it is acknowledged that the choice of sEMG-processing type may affect the
30 reliability of methodologies based on it. Analogously, the number of sEMG signals
31 involved in machine-learning procedure could influence the classification process. Aim
32 of this study is to quantify the impact of different EMG-signal-processing specifications
33 and/or different complexity of the experimental sEMG-protocol (different number of
34 sEMG-sensors) on the performance of a neural-network-based approach for binary
35 classifying gait phases and predicting gait-event timing. To this purpose, sEMG signals
36 are collected from eight leg-muscles in about 10.000 strides from 23 healthy adults during
37 walking and then fed to a multi-layer perceptron model. Four different signal-processing
38 approaches are tested and five experimental set-ups (from four to one sEMG sensors per
39 leg) are compared. Results indicate that both the choice of sEMG processing and the
40 reduction of sEMG-protocol complexity actually affect classification/prediction
41 performances. Moreover, the study succeeds in the double goal of identifying the linear
42 envelope as the sEMG-processing type which reaches the best neural-network
43 performance (classification accuracy of $93.4\pm 2.3\%$; mean absolute error 21.6 ± 7.0 and
44 38.1 ± 15.2 ms for heel-strike/toe-off prediction, respectively) and providing a
45 quantification of the progressive deterioration of classification/prediction performances
46 with the reduction of the number of sensors used (from $93.4\pm 2.3\%$ to $79.9\pm 6.1\%$ for
47 classification accuracy). These findings could be very useful for clinics to the aim of
48 choosing the most suitable approach balancing technical performances, patient comfort,
49 and clinical needs.

50

51 **1. Introduction**

52 Each single gait cycle of human walking is composed of two main phases: the stance
53 phase, from the beginning to around 60% of gait cycle; the swing phase, from 60% to the
54 end of gait cycle [1]. The stance phase denotes the whole time interval when the reference
55 foot is touching the ground. The swing phase quantifies the period when the foot is no
56 longer on the ground and swings in the air for leg advancement. Crucial for quantification
57 of gait phases duration are the transition events between the two phases: toe-off (TO,
58 from stance to swing) and heel-strike (HS, from swing to stance). The assessment of these
59 temporal parameters is one of the typical tasks of gait analysis [2,3].

60 In the recent years, artificial-intelligence techniques have been proposed for the
61 classification of stance vs. swing and for the assessment of temporal gait events [4,5].
62 Particularly valuable are those methodologies where machine and deep learning are
63 implemented with the aim of limiting the number of sensors involved in the experimental
64 set-up, such as electromyography-based approaches [6-12]. These studies are designed
65 to classify gait phases and predict gait events from only surface electromyographic signals
66 (sEMG), avoiding the requirement of directly measuring temporal data by means of
67 additional systems or sensors (foot-switch sensors, IMUs, pressure mats, stereo-
68 photogrammetry). This would allow to reduce burden for patient, simplify clinical
69 protocols, and make test faster, specifically in the evaluation of neuromuscular diseases
70 or for walking-aid devices where the acquisition of myoelectric signals is largely advised
71 [13,14]. The advantage would be even greater if it could be possible not only limiting the
72 number of sensors for temporal-data measurement, but also decreasing the number of
73 sEMG probes themselves. Obviously, reducing the number of sEMG sensors means
74 having fewer signals to be processed by the neural network. This is expected to lead to a
75 deterioration of classification performances. To our knowledge, a reliable analysis of the

76 effect on classification/prediction performance of the reduction of sEMG signals involved
77 in feeding the neural network is not yet available in literature.

78 Furthermore, the problem of gait-phase classification with neural-network-based
79 interpretation of only electromyographic signals has been typically faced extracting
80 explicit features from sEMG signal and then using them as input to the machine learning
81 stages [6-10]. The present group of researchers recently experimented a different strategy
82 [11,12], consisting in the application of neural networks to learn hidden features from a
83 processed sEMG signal. This strategy seems to improve the classification performances
84 [11], but at the same time it introduces the need of identifying the most suitable sEMG-
85 processing type. Recent studies, indeed, indicate that the choice of processing type and
86 processing-parameter value could be very subjective [15], could influence the reliability
87 of methodologies implemented to assess muscle activity [16], and could also affect the
88 estimation of gait events (HS and TO) [17]. Thus, the choice of the sEMG processing is
89 still an open issue.

90 The aim of the present study is to quantify the impact of different complexity of the
91 experimental sEMG-protocol (i. e. different number of sEMG sensors) and/or different
92 EMG-signal-processing specifications on the performance of a neural-network-based
93 approach for the binary classification of gait phases and prediction of gait-event (HS and
94 TO) timing. This aim is pursued, attempting to provide the following main contributions:

95 1) identifying which one of the following widely-used approaches to process EMG
96 signals allows to achieve the best classification/prediction performances: a) band-
97 pass filtered signal; b) full-wave rectified signal; c) linear envelope of the signal;
98 and d) root mean square signal. Details of these sEMG-signal processing are
99 reported in Section 3.3;

- 100 2) testing the sensitivity of the performances to different values of envelope cut-off-
101 frequency. Values of 5, 10, 15, and 20 Hz were adopted, considering that envelope
102 cut-off frequency typically ranges from 3 Hz to 25 Hz [15].
- 103 3) quantifying the conceivable decrease of classification/prediction performance
104 with the reduction of the number of sEMG signals involved in feeding the neural
105 network. Five experimental set-ups are considered to this purpose, including: 1)
106 sensors positioned on the proximal and distal leg (medial hamstrings, MH, vastus
107 lateralis, VL, tibialis anterior, TA, and gastrocnemius lateralis, GL, full set-up); 2)
108 only sensors positioned on the proximal leg (MH and VL, proximal leg set-up);
109 3) only sensors positioned on the distal leg (TA and GL, distal leg set-up); 4) only
110 sensors positioned on tibialis-anterior muscle (TA set-up); and 5) only sensors
111 positioned on gastrocnemius-lateralis muscle (GL set-up).

112 The manuscript is organized as follows: Section 2 provides a brief review of the related
113 works. Section 3 introduces the dataset, illustrates the acquisition and the pre-processing
114 of the signals, describes the procedure of gait-phase classification and gait-event
115 prediction by machine-learning approach, and presents the statistical tests. Section 4
116 reports the experimental results that are then discussed in Section 5. Both results and
117 discussion sections are split in two sub-sections about signal pre-processing and reduction
118 of experimental set-up, respectively. Eventually, Section 6 ends the study and provides
119 insights for further research developments.

120

121

122

123

124

125 **2. Related Works**

126 A relatively small number of works in literature address gait-phase classification
127 from EMG signals only. In [6] a set of time-domain features, namely mean absolute value
128 (MAV), waveform length (WL), zero crossing (ZC), and slope sign changes (SSC) were
129 extracted from EMG signal and hidden Markov models were used to classify stance and
130 swing phases. Evaluation on treadmill walking of a single subject reported a maximum
131 accuracy of 91.1%. Monitored muscles are Vastus Medialis, Semitendinosus, Adductors,
132 and Tensor Fascia Latae. A novel bilateral EMG feature, called weighted signal
133 difference (WSD), was introduced in [9] and used to train a support vector classifier
134 (SVC). Intra-subject evaluation is performed on two subjects walking on a treadmill at
135 different speed, reporting a best accuracy of 96%. Monitored muscles were Soleus,
136 Tibialis Anterior, Gastrocnemius Lateralis, Vastus Lateralis, Rectus Femoris and Gluteus
137 Maximus. In [7] a control system for a foot-knee exoskeleton based on the processing of
138 eight EMG signals is proposed. Four time-domain features (MAV, WL, Variance and
139 SGC) were extracted and Bayesian Information Criteria (BIC) was used to predict 8
140 distinct gait events. Evaluation on one healthy subject revealed low repeatability of the
141 method, with a 30% drop in accuracy testing on different gait cycles. Monitored muscles
142 were Quadriceps, Hamstring, Gastrocnemius and Tibialis Anterior. In [8] and [10] a set
143 of temporal features, namely root mean square (RMS), standard deviation (SD), MAV,
144 WL, and integrated EMG (IEMG), were fed to a single layer neural networks to detect
145 TO and HS on a population of 8 healthy adults. The study targets inter-subject prediction
146 by testing the network on one unlearned subject (not used in training), however no cross
147 validation is performed and the test is performed on a 5-second walk only. No indication
148 is provided regarding accuracy of prediction and a mean average error of 35 ms and 49

149 ms is reported for HS and TO prediction respectively. Monitored muscles were Tibialis
150 Anterior (TA) and Medial Gastrocnemius (mGas).

151 All the works mentioned above were based on explicit features extraction and used
152 different sets of features as input to the machine learning stage. Recently, a different
153 approach was introduced [11,12], where the original sEMG signal is first pre-processed,
154 in order to obtain a smoothed and cleaner signal, and then neural networks were used to
155 learn hidden features, classifying the two main gait phases and successively individuate
156 the TO and HS events as the transitions between different phases. The sEMG signals
157 acquired during level ground walking from eight lower-limb muscles, tibialis anterior
158 (TA), gastrocnemius lateralis (GL), medial hamstrings (MH), and vastus lateralis (VL) of
159 each leg, in more than 10.000 strides from 23 healthy adult subjects were involved [11].
160 As far as we know, this work is still reporting the best performances in HS and TO
161 prediction (mean absolute error of 21.6 ± 7.0 ms and 38.1 ± 15.2 ms, respectively and F1-
162 score $\approx 99\%$) among the mentioned sEMG-based studies. These promising results were
163 achieved by feeding the classifier with the envelope of EMG signal, computed as follows
164 [11]: sEMG signal was band-pass filtered (linear-phase FIR filter, cut-off frequency: 20
165 - 450 Hz), then full-wave rectified, and eventually the envelope was extracted (second-
166 order Butterworth low-pass filter, cut-off frequency: 5 Hz). Such a pre-processing
167 pipeline was designed following the indications provided by previous acknowledged
168 studies [18,19].

169

170 **3. Materials and Methods**

171 **3.1 Participants**

172 Twenty-three able-bodied adults were involved in the experimental procedure.
173 Volunteer data, reported as mean value \pm SD, are the following: height = 173 ± 10 cm;

174 mass = 63.3 ± 12.4 kg; age = 23.8 ± 1.9 years; and female/male ratio = 12/11. Subjects
175 with articular pain, with disorder of the nervous system, in obese or overweight condition
176 (body mass index > 25), and with history of orthopaedic surgery that may affect walking
177 performances were exempted from the study. The research presented here was undertaken
178 following the ethical principles of Helsinki Declaration and was approved by local ethical
179 committee.

180

181 **3.2 Signal acquisition**

182 The multichannel recording system Step32 (Medical Technology, Italy, Version PCI-
183 32 ch2.0.1. DV) was employed for signal acquisition (resolution: 12 bits; sampling rate:
184 2 kHz). Three foot-switches were placed under the heel, the first and the fifth metatarsal
185 heads of both subject's feet, for acquiring foot-floor-contact signal. Four sEMG sensors
186 were applied over vastus lateralis (VL), medial hamstrings (MH), tibialis anterior (TA),
187 and gastrocnemius lateralis (GL) of both legs, complying with recommendations
188 suggested by SENIAM standards [19]. After that, subject walked barefoot approximately
189 5 minutes on an eight-shaped path at her/his own pace. Experiments were performed in
190 Motion Analysis Laboratory of the Università Politecnica delle Marche, Ancona, Italy.
191 Characteristics of sEMG single-differential probes are: material = Ag/Ag-Cl disks; gain
192 = 1000, filtering = high-pass filter with cut-off frequency of 10 Hz; input impedance >
193 $1.5G\Omega$; Common-Mode Rejection Ratio > 126 dB; input referred noise $\leq 1 \mu V_{rms}$; and
194 manufacturer = Medical Technology, Italy. sEMG probes with fixed geometry have size
195 of $7 \times 27 \times 19$ mm; electrode diameter of 4 mm; and inter-electrode distance of 8 mm).
196 sEMG probes with variable geometry have a minimum inter-electrode distance of 12 mm.
197 Characteristics of foot-switches are: size = $11 \text{ mm} \times 11 \text{ mm} \times 0.5 \text{ mm}$ and activation
198 force = 3 N. Additional information about signal acquisition could be obtained in [20].

199 3.3 Signal pre-processing

200 Foot-switch signals were processed for recognizing gait cycles and stance/swing
201 phases [21]. To test the effect of signal filtering on classification performance, sEMG
202 signal were pre-processed with four different approaches.

203
204 *Band-pass filtered signal (BPFS)*: sEMG signals were band-pass filtered (linear-phase
205 FIR filter, cut-off frequency: 20 - 450 Hz) for taking out high frequency noise and motion
206 artefacts.

207
208 *Full-wave Rectified signal (FWRS)*: sEMG signals were band-pass filtered (linear-phase
209 FIR filter, cut-off frequency: 20 - 450 Hz). Then, a full-wave rectification was achieved,
210 taking the absolute value of the signal.

211
212 *Linear envelope of the signal (LE)*: sEMG signals were band-pass filtered (linear-phase
213 FIR filter, cut-off frequency: 20 - 450 Hz) and full-wave rectified. Then, envelope of the
214 signal was extracted (second-order Butterworth low-pass filter). Four different values of
215 cut-off frequency were tested: 5, 10, 15, and 20 Hz. These four different processing of
216 the envelope have been referred to as LE_5 , LE_{10} , LE_{15} , and LE_{20} , respectively.

217
218 *Root mean square signal (RMSS)*: sEMG signals were band-pass filtered (linear-phase
219 FIR filter, cut-off frequency: 20 - 450 Hz). Then, a sliding window of length N scans the
220 signal sample by sample. $RMSV$ computed in the first window is the first sample of the
221 Root mean square signal. $RMSV$ computed in the second window is the second sample of
222 the Root mean square signal and so on. $RMSV$ is computed as in the following formula:

223

$$224 \quad RMSV = \sqrt{\frac{1}{N} \sum_{k=1}^N |x_k|^2} \quad (1)$$

225

226 where N is number of samples, x_k is the k -sample. Two different values of sliding-window
227 duration were tested: 100 samples ($RMSS_{100}$) and 500 samples ($RMSS_{500}$). After every
228 kind of filtering, sEMG signals were min-max normalized within each subject and for
229 each muscle, thus mapping the values in the $[0-1]$ interval. All the pre-processing
230 operations were implemented using Matlab relying on standard functions provided by the
231 Signal Processing Toolbox¹.

232

233 **3.4 Data preparation**

234 Each sEMG signal was separated into 20-sample windows, matching 10 milliseconds
235 (ms). A chronological sequence of vectors made up of $20 \times n$ samples was composed,
236 where each vector included n synchronized 20-sample windows from sEMG signals of n
237 muscles ($n/2$ for each leg). In details, the first sample of the first vector of the sequence
238 was the first sample of the sEMG signal from the muscle 1 (TA, right leg), the second
239 sample of the first vector was the first sample of the EMG signal from the muscle 2 (GL,
240 right leg), and so on up to the muscle n . After that, each vector was given a specific label
241 of 0 (or 1), when all basographic-signal samples assume a value of 0 (or 1). Vectors
242 containing transitions between phases were not included in the training set.

243 The classifier was then trained following the leave-one-out cross validation
244 procedure: 22 out of 23 subjects were involved in training the classifier (Learned subjects,
245 LS); the remaining subject was employed to test the classification output (Unlearned
246 subject, US). LS were further separated into two subsets: training set containing the first
247 90% of each subject signal (LS-train); testing set including the remaining 10% (LS-test).

¹ <https://it.mathworks.com/products/signal.html>

248 In details, the classifier was fed with the vectors extracted from LS-train. The vectors
249 from US and LS-test were employed for testing the classifier performances in unseen
250 subject and in unseen samples of learned subjects, respectively. In this stage, foot-switch
251 signal was the ground truth. This process has been repeated twenty-three times, each time
252 employing a different subject as US.

253

254 **3.5 The neural network**

255 A Multi Layer Perceptron (MLP) classifier was used in the present study. The MLP
256 architecture is characterized by:

- 257 • 3 hidden layers of 512, 256 and 128 neurons, respectively;
- 258 • a one-dimensional binary output, provided by applying a 0.5 threshold to a
259 sigmoid activation;
- 260 • a rectified linear units (ReLU) between each couple of consecutive hidden
261 layers to supply non-linearity;
- 262 • a stochastic gradient descent optimization algorithm with binary cross
263 entropy loss function.

264 The specific architecture was chosen among others, with different numbers of layers,
265 tested in [11], as it provided the best classification accuracy. In training the network, 10%
266 of the training dataset was used as validation set. At each training epoch, accuracy on the
267 validation set is measured and training was stopped when the validation accuracy did not
268 increase in 10 consecutive epochs. Then, the trained network weights, corresponding to
269 the best validation accuracy, were used to evaluate the model on the LS-test and US sets.

270 The neural network and the corresponding training and testing code were implemented in
271 Python using the Pytorch deep learning framework² and the Scikit-Learn python library³.

272

273 **3.6 Gait-event identification**

274 The binary output of the classifier has been chronologically arranged to provide the
275 predicted foot-floor-contact signal, as a vector made up of sequences of 0 (stance phase)
276 alternating with sequences of 1 (swing phase). While signal windows containing
277 transitions were discarded in the training phase, all of them were fed as input to the
278 classifier, in order to predict the foot-floor-contact signal. It is acknowledged that stance
279 and swing are typically lasting around 60% and 40% of gait cycle, during able-bodied
280 walking [1]. Accordingly, the sample sequences shorter than 500 samples (< 25% of gait
281 cycle) were removed to clean out the predicted signal. Afterward, stance-to-swing (toe
282 off, TO) and swing-to-stance (heel strike, HS) transitions have been assessed in the
283 cleaned signal. TO was identified as the sample when the value switched from 0 to 1.
284 Similarly, HS was identified as the sample when the value switched from 1 to 0.
285 Prediction performances were quantified in terms of precision, recall, and F1-score.
286 Precision is computed as:

$$287 \quad \textit{Precision} = \frac{TP}{TP + FP} \quad (2)$$

288

289 where *TP* is true positive and *FP* is false positive. Recall is computed as:

290

² <https://pytorch.org/>

³ <https://scikit-learn.org/stable/>

291
$$Recall = \frac{TP}{TP + FN} \quad (3)$$

292

293 where FN is false negative. F1-score is computed as:

294

295
$$F1 - score = 2 \cdot \frac{Precision \cdot Recall}{Precision + Recall} \quad (4)$$

296

297 Predicted HS or TO at time t_p were acknowledged as true positives (TP) if an event of the
298 same type occurs in ground-truth signal at time t_g such that $|t_g - t_p| < T$. T is a time
299 tolerance, set to 600 samples. Otherwise, the predicted event was acknowledged as a false
300 positive (FP). For all TP , mean absolute error (MAE) has been computed, as the mean
301 time distance between the predicted event and the corresponding event in ground-truth
302 signal.

303

304 **3.7 Statistics**

305 Shapiro-Wilk test was used to evaluate the hypothesis that each data vector had a
306 normal distribution. Comparison between two normally distributed samples was
307 performed with two-tailed, non-paired Student's t-test. Two-sample Kolmogorov-
308 Smirnov test was used to compare not normally distributed samples. Statistical
309 significance was set at 5%.

310

311

312

313

314 4. Results

315 4.1 Signal pre-processing

316 Average classification accuracies as result of different pre-processing of the signal
317 are reported in Table 1, for Learned-test set (LS-test) and Unlearned set (US). Linear
318 envelope (*LE*) of the signal is evaluated considering four different values of cut-off
319 frequency: 5, 10, 15, and 20 Hz.

320

321 **Table 1.** Mean classification accuracy as result of
322 different pre-processing of the signal.

Mean classification accuracy (%)		
	LS-test	US
<i>LE</i> ₅	94.8 ± 0.2	93.4 ± 2.3
<i>LE</i> ₁₀	93.8 ± 0.3	93.1 ± 2.4
<i>LE</i> ₁₅	93.2 ± 0.3	91.4 ± 2.4
<i>LE</i> ₂₀	92.4 ± 0.4	90.3 ± 3.3
<i>RMSS</i> ₁₀₀	92.3 ± 0.5	90.1 ± 2.9
<i>RMSS</i> ₅₀₀	93.0 ± 0.4	91.0 ± 3.7
<i>FWRS</i>	88.8 ± 0.2	88.0 ± 2.9
<i>BPFS</i>	86.5 ± 0.6	84.0 ± 3.7

323

324

325 Classification results highlight that accuracy is decreasing with increasing cut-off
326 frequency in both LS-test (from 94.8% to 92.4%) and US (from 93.4% to 90.3%). In a
327 similar way, SD is increasing with increasing cut-off frequency (from 0.2 to 0.4 in LS-
328 test; from 2.3 to 3.3 in US). Comparison between Root mean square signals (*RMSS*)
329 computed with two different values of sliding-window duration shows slightly better
330 accuracy for *RMSS*₅₀₀ for both LS-test and US. All *LE* and *RMSS* approaches report a
331 mean classification accuracy > 92% in LS-test and > 90% in US. Otherwise, *FWRS* and

332 *BPFS* approaches remain definitely $< 90\%$, in particular for US. Overall, best mean
 333 accuracy (and SD) is provided by LE_5 in both LS-test and US.

334

335 **Table 2.** MAE (mean absolute error), precision, recall, and F1-score as result
 336 of different pre-processing of the signal for Heel Strike (HS) and Toe Off
 337 (TO) prediction in US.

Mean prediction performances				
Heel Strike (HS)	MAE (ms)	Precision (%)	Recall (%)	F1-score (%)
LE_5	21.6 ± 7.0	99.7 ± 0.6	98.5 ± 3.0	99.0 ± 1.7
LE_{10}	26.7 ± 9.8	99.6 ± 0.7	98.8 ± 1.6	99.2 ± 1.1
LE_{15}	27.4 ± 11.7	99.5 ± 0.6	98.7 ± 1.3	99.1 ± 0.9
LE_{20}	35.1 ± 26.5	98.9 ± 2.5	98.1 ± 3.3	98.5 ± 2.8
$RMSS_{100}$	28.1 ± 9.6	99.2 ± 1.2	98.0 ± 3.0	98.6 ± 1.9
$RMSS_{500}$	33.9 ± 14.3	98.7 ± 2.2	98.1 ± 2.6	98.4 ± 2.3
$FWRS$	47.3 ± 24.9	99.2 ± 1.0	98.4 ± 1.8	98.9 ± 1.4
$BPFS$	77.4 ± 40.4	95.6 ± 5.9	90.4 ± 13.0	92.6 ± 9.7
Toe Off (TO)	MAE (ms)	Precision (%)	Recall (%)	F1-score (%)
LE_5	38.1 ± 15.2	99.1 ± 1.5	97.9 ± 3.6	98.4 ± 2.4
LE_{10}	46.0 ± 22.6	98.7 ± 2.3	97.9 ± 2.9	98.3 ± 2.5
LE_{15}	47.9 ± 19.3	98.4 ± 2.3	97.6 ± 2.7	98.0 ± 2.4
LE_{20}	58.2 ± 26.4	98.5 ± 2.1	97.6 ± 2.8	98.0 ± 2.4
$RMSS_{100}$	58.3 ± 22.3	98.6 ± 1.9	97.4 ± 3.6	97.9 ± 2.7
$RMSS_{500}$	54.1 ± 29.5	97.8 ± 3.2	97.1 ± 3.6	97.5 ± 3.4
$FWRS$	58.8 ± 29.9	97.3 ± 5.0	96.5 ± 5.3	96.9 ± 5.1
$BPFS$	67.7 ± 25.6	97.6 ± 3.1	92.2 ± 11.4	94.5 ± 7.8

338

339

340

341 Performances in assessing HS and TO events in US are reported in Table 2, in terms
342 of MAE, precision, recall, and F1-score. LE_5 provides the best MAE in HS and TO
343 identification in US, in terms of both mean and SD (21.6 ± 7.0 ms and 38.1 ± 15.2 ms,
344 respectively). Even LE_{10} , LE_{15} , and $RMSS_{100}$ are able to keep HS-MAE value < 30 ms,
345 but they fail in keeping TO-MAE value < 40 ms. All LE and $RMSS$ approaches are able
346 to maintain precision, recall and F1-score $> 98\%$ for HS and $> 97\%$ for TO. $FWRS$ and
347 $BPFS$ approaches supply the worst performances. Average performances in every subject
348 are reported in supplementary material 1-8.

349 All experiments run on a machine equipped with a 2,6 GHz Intel Core i7 processor,
350 16 GB RAM. The best performing signal pre-processing pipeline (LE_5) required
351 approximately 70 milliseconds in average to process a 1-second signal. It then took
352 around 0.2 milliseconds for the neural network to process and predict gait events for a
353 single pre-processed signal window (20 samples). In conclusion, the total processing time
354 sums up to 90 milliseconds to predict TO and HS events for a 1 second walk. In the
355 present experiments, the network training time over 22 training subjects (one single fold)
356 ranges from approximately 30 minutes, when the simpler experimental protocol is
357 adopted (a single EMG signal per leg, two in total) to approximately 60 minutes, when
358 all the four EMG signals per leg (eight in total) are used. However, we also note that the
359 network training has to be done only once, then the trained network can be applied as-is
360 to predict TO and HS in unseen subjects.

361

362 **4.2 Reduction of experimental set-up**

363 Since it turned out to be the best-performing processing technique, LE_5 has been used
364 to perform the analysis of the reduction of experimental set-up. Average classification
365 accuracies as a result of different experimental set-ups are reported in Table 3, for

366 Learned-test set (LS-test) and Unlearned set (US). The full protocol (reference) provides
367 the best classification accuracy ($94.8 \pm 0.2\%$ for LS-test and $93.4 \pm 2.3\%$ for US). In the
368 distal-leg approach, a significant ($p < 0.05$) decrease of 2 percentage points of
369 classification accuracy is detected for both LS-test and US, compared to the reference.
370 However, accuracy is still widely $> 90\%$. The gap from the reference further increases (p
371 < 0.05), considering the single muscles (GL and TA) and the proximal-leg approach
372 (Table 3). Performances in assessing HS and TO events in US are reported in Table 4, in
373 terms of MAE, precision, recall, and F1-score. The full protocol supplies the best MAE
374 in HS and TO identification in US, in terms of both mean and SD (21.6 ± 7.0 ms and 38.1
375 ± 15.2 ms, respectively) and the best F1-score ($99.0 \pm 1.7\%$ and $98.4 \pm 2.4\%$). A
376 significant worsening in HS-MAE ($\approx + 10$ ms, $p < 0.05$) is detected in prediction of distal-
377 leg and GL approaches.

378
379

380
381

Table 3. Mean classification accuracy as result of different experimental set-ups

Mean classification accuracy (%)		
	LS-test	US
Full	94.8 ± 0.2	93.4 ± 2.3
Proximal leg	84.6 ± 0.9	79.9 ± 6.1
Distal leg	92.6 ± 0.3	91.4 ± 2.6
GL	88.4 ± 0.5	89.1 ± 3.6
TA	86.9 ± 0.4	84.6 ± 6.9

382
383
384
385
386
387
388
389
390

391
392
393

Table 4. MAE (mean absolute error), precision, recall, and F1-score as result of different experimental set-ups for Heel Strike (HS) and Toe Off (TO) prediction in US.

Mean prediction performances				
Heel Strike (HS)	MAE (ms)	Precision (%)	Recall (%)	F1-score (%)
Full	21.6 ± 7.0	99.7 ± 0.6	98.5 ± 3.0	99.0 ± 1.7
Proximal leg	52.9 ± 23.8	96.3 ± 5.0	90.0 ± 9.3	92.8 ± 6.5
Distal leg	33.2 ± 13.1	99.5 ± 0.7	97.3 ± 4.6	98.3 ± 2.7
GL	33.0 ± 12.0	99.7 ± 0.4	96.5 ± 6.7	98.0 ± 4.1
TA	53.6 ± 38.4	95.5 ± 6.1	83.8 ± 15.1	88.7 ± 10.9

Toe Off (TO)	MAE (ms)	Precision (%)	Recall (%)	F1-score (%)
Full	38.1 ± 15.2	99.1 ± 1.5	97.9 ± 3.6	98.4 ± 2.4
Proximal leg	71.2 ± 24.4	92.3 ± 11.0	86.1 ± 11.9	88.9 ± 10.7
Distal leg	45.1 ± 18.7	98.6 ± 2.0	96.4 ± 5.0	97.5 ± 3.3
GL	64.6 ± 25.8	98.9 ± 1.5	95.7 ± 6.7	97.1 ± 4.1
TA	49.0 ± 16.6	95.7 ± 5.7	83.9 ± 15.5	88.8 ± 11.1

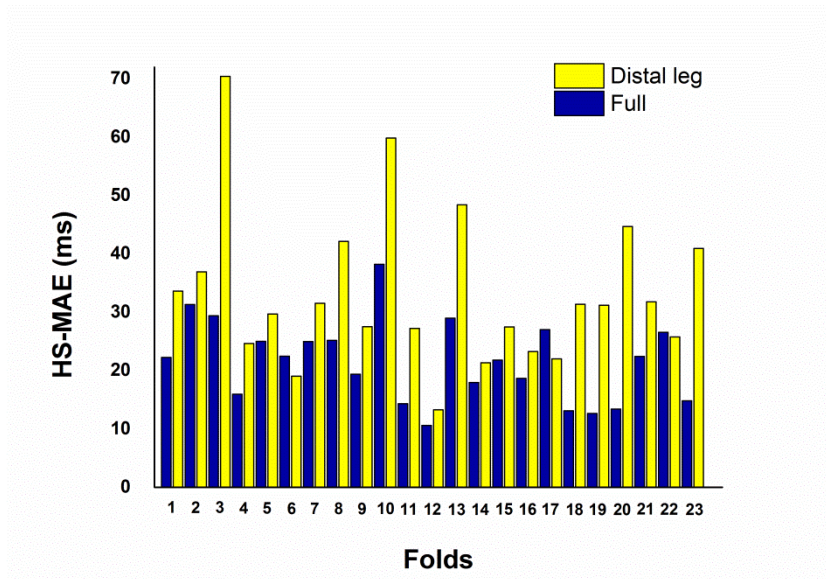
394

395

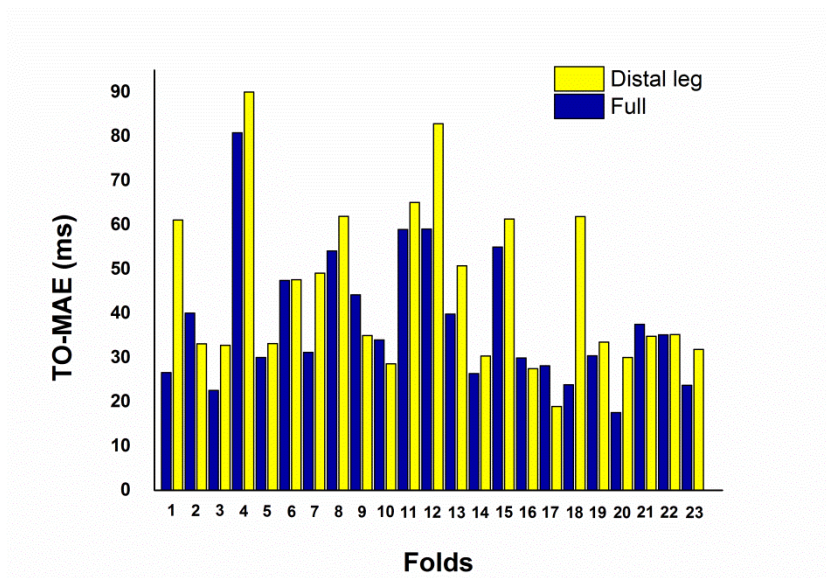
396 A further increase of MAE ($\approx + 20$ ms, $p < 0.05$) and decrease of F1-score (from 6%
397 to 10%) were predicted by the other two approaches. TO-MAE worsens in prediction of
398 distal-leg and TA approaches (≈ 7 and 11 ms, respectively), even if not significantly ($p >$
399 0.05). A concomitant decrease of F1-score is detected ($\approx -1\%$). Further remarkable
400 worsening of both parameters was reported for the other two approaches. Figure 1 shows
401 a direct comparison between the accuracy provided by distal-leg (yellow bars) vs.
402 reference set-up (full, blue bars) in each fold. Average performances in every subject are
403 reported in supplementary material 9-12.

404

405



406



407

408

409

410

411

Fig. 1. Direct comparison of MAE provided in each fold by full set-up (dark blue bars) vs. distal-leg set-up (yellow bars) for HS (upper panel) and TO (lower panel) predictions.

412

413

414 5. Discussion

415

416

417

The present group of researchers recently proposed a neural-network-based approach for classifying stance vs. swing and assessing temporal gait events from electromyographic signals [11]. A twofold objective is pursued in the present study, i.e.

418 to test the influence on the performance of the above-mentioned approach of: 1) different
419 pre-processing of sEMG signal; 2) reduction of the number of sEMG probes included in
420 the experimental set-up. The approach described in [11] was chosen as reference model,
421 because to our knowledge it is still outperforming all similar studies in terms of HS and
422 TO prediction [6-10]. Foot-switch signal was adopted as the ground truth, since it
423 represents the gold standard in gait segmentation [21-23].

424

425 **5.1 Signal pre-processing**

426 The first step was to test if the change of low-pass cut-off frequency for extracting
427 the envelope could affect classification and/or prediction performances. Average results
428 show that classification accuracy (Table 1) and prediction MAE (Table 2) gradually
429 worsen with concomitantly increasing cut-off-frequency value (starting from the
430 reference value of 5 Hz), in terms of both mean value and SD. These results clearly show
431 that the performances of the classifier are affected by the choice of the cut-off-frequency
432 and 5 Hz is the best value for the goal we set. This suggests that when the envelope of
433 sEMG signal is used, the cut-off-frequency value should be carefully evaluated in relation
434 to the adopted methodology and pursued aim, in order to avoid estimation bias, as shown
435 for co-contraction assessment in [16].

436 The second step was to compare the performances of the classifier after feeding the
437 neural network with sEMG signal filtered in different ways. The simplest filter analyzed
438 is *BPFS*, because it is necessary for removing low-frequency motion artefacts and high-
439 frequency noise from the signal. This approach returns the worst mean and single-subject
440 (see supplementary material 8) classification accuracy among the approaches considered
441 in the present study, especially for the unseen subjects (mean \pm SD = 84.0 \pm 3.7%, Table
442 1). The worst performances are provided also in the assessment of gait events (Table 2).

443 *BPFS* is the only approach not performing the rectification of the signal. Thus, these
444 findings indicate that the full-wave rectification is strongly recommended in processing
445 the signal to feed the neural network. However, the full-wave rectification alone does not
446 seem to be enough. *FWRS* approach truly improves *BPFS* one, but accuracy is still < 90%.
447 Moreover, the performances are far from the ones provided by more refined processing
448 approaches, such as *LE* and *RMSS* (Table 1 and 2). All *LE* and *RMSS* approaches, indeed,
449 report a mean classification accuracy > 90% (Table 1) and keep mean precision, recall
450 and F1-score > 98% for HS and > 97% for TO (Table 2). Furthermore, the best performing
451 *LE* approach (*LE*₅) outperforms also the *RMSS* approaches, above all in terms of average
452 classification accuracy ($\approx 95\%$ in learned subjects and $> 93\%$ in unseen subjects), HS-
453 MAE (21.6 ± 7.0 ms vs. 28.1 ± 9.6 ms provided by the best performing *RMSS* approach),
454 and TO-MAE (38.1 ± 15.2 ms vs. 54.1 ± 29.5 ms). About *RMSS*, the different durations
455 of sliding-window do not seem to influence the classifier performance.

456 In the end, present results confirm that the choice of the sEMG processing actually
457 affects the classification/prediction performances, as expected [15-17]. Moreover, the
458 present study succeeds in identifying the linear envelope (cut-off frequency 5 Hz) as the
459 sEMG-processing type which provides the best performance of the neural network in
460 terms of both classification accuracy and gait-event-prediction, among the four widely-
461 used approaches analyzed in the present study. This methodological finding, reported
462 here for the first time, is very useful information for improving the precision of the clinical
463 test by means of the most adequate processing of the signal. It seems especially valuable
464 for those clinical conditions (such as neurological disorders) where elevated precision of
465 predictions is fundamental to properly identify subject recovery during follow-up.

466

467

468 **5.2 Reduction of experimental set-up**

469 Since LE_5 is resulted being the best-performing approach for the sEMG-signal
470 processing, it was used to run the analysis of the reduction of experimental set-up, i.e. the
471 number of sEMG probes. Besides the full protocol [11], four reduced experimental set-
472 ups are considered in the present paper, in order to test the influence of protocol
473 simplification on classification/prediction performances. The first step was to test if the
474 reduction from four to two sEMG sensors per leg could provide classification/prediction
475 results consistent with those provided by the full set-up. Two attempts were made, using
476 signals from a couple of sensors applied to the same leg segment (proximal or distal), one
477 in the front and one in the back. Table 3 shows as mean classification accuracy provided
478 by the proximal-leg set-up clearly deteriorates compared to the full set-up, falling below
479 85% in learned subjects and below 80% in unseen ones. This is also more evident by
480 analysing each single subject, as reported in supplementary material 9. The proximal-leg-
481 based reduction of the number of sensors strongly affects also MAE, precision, recall,
482 and F1-score, especially in TO prediction (MAE = 71.2 ± 24.4 ms and F1-score < 90%,
483 Table 4). The matter is different for the distal-leg set-up. Although a decrease of mean
484 classification accuracy is still detected, it amounts to only 2 percentage points in both
485 learned ($92.6 \pm 0.3\%$) and unseen subjects ($91.4 \pm 2.6\%$). Moreover, precision, recall, and
486 F1-score remain practically unaltered. The mean increase of MAE compared to the full
487 set-up (+ 11.6 ms for HS; + 7.0 ms for TO, Table 4) is the price to pay for using only two
488 probes per leg. For allowing a more detailed evaluation, MAEs provided by the two set-
489 ups in each single subject are compared in Fig. 1. These findings show as the distal-leg
490 set-up clearly outperforms the proximal-leg one in terms of all performance parameters.
491 To our knowledge, only Nazmi et al. [10] provided neural-network prediction of gait
492 events using only two sEMG probes per leg on distal-leg muscles (tibialis anterior and

493 gastrocnemius medialis). They achieved, for unseen subjects, a mean classification
494 accuracy of 77% and MAE of 35 ms and 49 ms in assessing HS and TO, respectively.
495 Compared to those, the present distal-leg-set-up results appear promising, considering
496 also that in present study F1-score is around 98%, while in [10] this information is not
497 reported. It is worth mentioning that in [10] HS and TO predictions are computed in only
498 5 seconds of a single subject, whereas in the present study an extensive evaluation is
499 performed, predicting HS and TO in a 5-minute walking of 23 different subjects (with
500 leave-one-out cross validation).

501 The second step was to test the effect of a further reduction to a single muscle of
502 experimental set-up. Considering the promising results achieved, two further attempts
503 were made, using signals from one sensor applied to a single muscle, in the front (TA) or
504 in the back (GL) of the distal leg. The results shown in Table 3 highlight that phase
505 classification based on a single sEMG signal leads to a deterioration of mean accuracy,
506 compared to both full and distal-leg set-ups. This is true for both TA (- 8% in learned and
507 - 7% in unseen subjects, compared to the full protocol) and GL set-ups (- 6% in learned
508 and - 4% in unseen subjects), although GL set-up achieves better accuracy, getting close
509 to 90% in unseen subjects. However, classification accuracies are still better than the ones
510 provided by the proximal-leg set-up and in [10]. TA and GL set-ups work differently in
511 HS and TO prediction. Compared to full set-up, mean precision, recall, and F1-score
512 remain practically unaltered for GL set-up. Prediction of TA set-up is instead affected by
513 a strong decrease of mean recall value (-14% and -12% compared to full and GL set-ups,
514 respectively). This means that a high number of false positive detection of HS and TO
515 affects the prediction. Consequently, a concomitant deterioration of F1 score is observed
516 (-10% and -9% compared to full and GL set-ups, respectively). HS prediction provided
517 by GL set-up presents a mean increase of MAE compared to the full set-up, but achieves

518 the same value provided by distal-leg set-up (33.0 ± 12.0 ms vs. 33.2 ± 13.1 ms).
519 Furthermore, mean HS-MAE is still comparable with the one reported in [10], using two
520 distal-leg muscles. TA set-up reports a significant growth of mean HS-MAE compared
521 to full (+33 ms), distal-leg (+20 ms), and GL (+20 ms) set-ups. These findings seem to
522 indicate that between GL and TA signals, only GL-signal plays a fundamental role in
523 prediction of heel strike. TO prediction is less accurate in GL-set-up (+26 ms and +19
524 ms of mean MAE compared to full and distal-leg set-ups, respectively). Larger MAEs in
525 TO prediction were foreseen, since it was explained that it is more challenging to assess
526 TO than HS [10,24]. On average, TO-MAE is lower for TA set-up ($49.0 \pm 16.6\%$,
527 comparable with distal-leg set up). However, as already mentioned, it is associate to low
528 performances in terms of classification accuracy ($84.6 \pm 6.9\%$), recall ($83.9 \pm 15.5\%$),
529 and F1-score ($88.8 \pm 11.1\%$). Thus, in our opinion TA-set-up-based prediction should be
530 considered not reliable and the desirable simplification of experimental set-up (one single
531 sensor) should involve only the GL set-up. In this case, this simplification would be paid
532 with a deterioration of TO (not HS) prediction. This could be a good compromise for
533 tasks such as stride recognition, stride-time computation, identification of toe walking,
534 and so on, where only HS event is involved.

535 In the end, present findings indicate that the reduction of the complexity of the
536 experimental sEMG-protocol (i. e. decreased number of sEMG sensors) affects the
537 performances especially in terms of gait-event-prediction parameters, as expected [10].
538 Moreover, the present study succeeds in the goal of providing for the first time a
539 quantification of the progressive deterioration of classification/prediction performances
540 with the reduction of the number of sensors used. This could be very useful in clinics to
541 the aim of choosing the most suitable approach, balancing technical performances, patient
542 comfort, and clinical needs. Since a simplification of experimental set-up is always

543 desirable, the present study proposes the distal set-up (consisting of two sensors over TA
544 and GL per leg) as a suitable alternative to the full protocol in those circumstances where
545 limiting time consumption and patient discomfort is a primary issue. The price to pay for
546 this simplification is essentially a worsening of HS and TO prediction (about 10 ms, on
547 average). A further reduction of experimental set-up to a single muscle seems to be
548 feasible without a further deterioration of performances only if GL is chosen as the
549 reference muscle and for computation where only heel-strike events are involved.

550

551

552 **6. Conclusions**

553 The present study shows that both the sEMG-processing type and the reduction of
554 sEMG-protocol complexity actually affect the performances of neural-network-based
555 classification of gait phases and assessment of temporal gait events. A further novel
556 contribution is to provide also a reliable quantification of this performance deterioration.
557 The quantitative knowledge of the consequences of the reduction of the number of sensors
558 in terms of classification/prediction accuracy could be very useful in clinics to drive the
559 choice of the most suitable experimental set-up for gait analysis, able to balance the need
560 of handling patient comfort and limiting time consumption with the necessity of
561 maintaining an elevated precision of test results. Higher precision in gait event prediction
562 is increasingly requested in clinics, especially in those pathologies where one of the gait
563 phases could be strongly reduced (neurological disorders). The present study provides
564 also the information about the most suitable sEMG-processing type (linear envelope with
565 a cut-off frequency = 5 Hz) to satisfy this necessity.

566 Four acknowledged and widely-used approaches to process EMG signals were
567 included in the present comparative analysis. Future development could be designed to

568 involve more advanced signal-processing techniques in frequency or time/frequency
569 domain, such as Fourier transform or wavelet transform. Moreover, the potential
570 influence of gait velocity could be also taken into account. This would be an intriguing
571 further direction, as EMG envelopes show adaptations to different gait velocities.

572

573

574 **References**

- 575 1. Perry J. Gait Analysis - Normal and Pathological Function. USA: Slack Inc, 1992.
- 576 2. Bovi G, Rabuffetti M, Mazzoleni P, Ferrarin M. A multiple-task gait analysis
577 approach: Kinematic,kinetic and EMG reference data for healthy young and adult
578 subjects. Gait Posture. 2011;33;6–13.
- 579 3. Caldas R, Mundt M, Potthast W, Buarque de Lima Neto F, Markert B. A systematic
580 review of gait analysis methods based on inertial sensors and adaptive algorithms.
581 Gait Posture. 2017;57;204–210.
- 582 4. Taborri J, Palermo E, Rossi S, Cappa P. Gait Partitioning Methods: A Systematic
583 Review. Sensors (Basel) 2016;16(1):66. doi: 10.3390/s16010066
- 584 5. Di Nardo F, Morbidoni C, Cucchiarelli A, Fioretti S. Recognition of Gait Phases with
585 a Single Knee Electrogoniometer: A Deep Learning Approach . Electronics
586 2020;9(2);355. <https://doi.org/10.3390/electronics9020355>
- 587 6. Meng M, She Q, Gao Y, Luo Z. EMG signals based gait phases recognition using
588 hidden Markov models. In Proceedings of the 2010 IEEE International Conference
589 on Information and Automation, Harbin, China, 20–23 June 2010; pp. 852–856.

- 590 7. Joshi CD, Lahiri U, Thakor NV. Classification of gait phases from lower limb EMG:
591 Application to exoskeleton orthosis. In Proceedings of the 2013 IEEE Point-of-Care
592 Healthcare Technologies (PHT), Bangalore, India, 16–18 January 2013:228–231.
- 593 8. Nazmi N, Abdul Rahman M, Ariff MHM, Ahmad S. Generalization of ANN Model
594 in Classifying Stance and Swing Phases of Gait using EMG Signals. In Proceedings
595 of the IEEE-EMBS Conference on Biomedical Engineering and Sciences (IECBES
596 2018), Sarawak – Kuching, Malaysia 3-6 December. 2018: 461-466.
- 597 9. Ziegler J, Gattringer H, Mueller A. Classification of Gait Phases Based on Bilateral
598 EMG Data Using Support Vector Machines. In Proceedings of the IEEE RAS and
599 EMBS International Conference on Biomedical Robotics and Biomechanics,
600 Enschede, The Netherlands, 26–29 August. 2018:978–983.
- 601 10. Nazmi N, Abdul Rahman M, Yamamoto SI, Ahmad S. Walking gait event detection
602 based on electromyography signals using artificial neural network. *Biomed Signal
603 Process Control*. 2019;47:334–343.
- 604 11. Morbidoni C, Cucchiarelli A, Fioretti S, Di Nardo F. A Deep Learning Approach to
605 EMG-Based Classification of Gait Phases during Level Ground Walking. *Electronics*
606 2019;8(8):894. <https://doi.org/10.3390/electronics8080894>
- 607 12. Morbidoni C, Principi L, Mascia G, Strazza A, Verdini F, Cucchiarelli A, Di Nardo
608 F. Gait Phase Classification from Surface EMG Signals Using Neural Networks. In:
609 Henriques J, Neves N, de Carvalho P (eds). XV Mediterranean Conference on
610 Medical and Biological Engineering and Computing - MEDICON 2019.
- 611 13. Kamruzzaman J, Begg RK. Support vector machines and other pattern recognition
612 approaches to the diagnosis of cerebral palsy gait. *IEEE Trans Biomed Eng.*
613 2006;53(12 Pt 1):2479-90.

- 614 14. Tang Z, Zhang K, Sun S, Gao Z, Zhang L, Yang Z. An upper-limb power-assist
615 exoskeleton using proportional myoelectric control. *Sensors (Basel)*.
616 2014;10;14(4):6677-94.
- 617 15. Rosa MC, Marques A, Demain S, Metcalf CD, Rodrigues J. Methodologies to assess
618 muscle co-contraction during gait in people with neurological impairment – a
619 systematic literature review. *J Electromyogr Kinesiol*. 2014; 24(2):179–191.
- 620 16. Rinaldi M, D'Anna C, Schmid M, Conforto S. Assessing the influence of SNR and
621 pre-processing filter bandwidth on the extraction of different muscle co-activation
622 indexes from surface EMG data. *J Electromyogr Kinesiol*. 2018;43:184-192. doi:
623 10.1016/j.jelekin.2018.10.007.
- 624 17. Caramia C, De Marchis C, Schmid M. Optimizing the Scale of a Wavelet-Based
625 Method for the Detection of Gait Events from a Waist-Mounted Accelerometer under
626 Different Walking Speeds. *Sensors (Basel)*. 2019;19(8):1869.
- 627 18. Winter DA, Yack HJ. EMG profiles during normal human walking: stride-to-stride
628 and inter-subject variability. *Electroencephalogr Clin Neurophysiol*.
629 1987;67(5):402-411.
- 630 19. Hermens HJ, Freriks B, Merletti R, et al. European recommendations for surface
631 electromyography, SENIAM. Enschede (NL): Roessingh Research and
632 Development 1999, 8.
- 633 20. Di Nardo F, Mengarelli A, Maranesi E, Burattini L, Fioretti, S. Gender differences
634 in the myoelectric activity of lower limb muscles in young healthy subjects during
635 walking. *Biomed Signal Process Control*. 2015;19:14–22.
- 636 21. Agostini V, Balestra G, Knaflitz M. Segmentation and Classification of Gait Cycles,
637 *IEEE Trans. Neural Syst. Rehabil. Eng*. 2014;22(5):946-52.

- 638 22. Taborri J, Palermo E, Rossi S, Cappa P. Gait partitioning methods: A systematic
639 review. *Sensors*. 2016;16:66.
- 640 23. Winiarski S, Rutkowska-Kucharska A. Estimated ground reaction force in normal
641 and pathological gait. *Acta Bioeng. Biomech*. 2009;11:53–60.
- 642 24. Khandelwal S, Wickstrasm N. Evaluation of the performance of accelerometer-based
643 gait event detection algorithms in different real-world scenarios using the MAREA
644 gait database. *Gait Posture*. 2017;51:84–90.